 doi:10.20944/preprints202009.0296.v1

Photocatalytic Nanocomposite Materials Based on Inorganic Polymers (Geopolymers): A Review.

Mahroo Falah[1], and Kenneth J.D. MacKenzie[2*],

1 Fiber and Particle Engineering Research Unit, Faculty of Technology, University of Oulu, 90014 Oulu, Finland; mahroo.falahpoorsichani@oulu.fi
2 MacDiarmid Institute for MacDiarmid Institute for Advanced Materials and Nanotechnology, School of Chemical and Physical Sciences, Victoria University of Wellington, New Zealand; kenneth.mackenzie@vuw.ac.nz

* Correspondence: Kenneth.mackenzie@vuw.ac.nz

Abstract.

Geopolymers are ecologically-friendly inorganic materials which can be produced at low temperatures from industrial wastes such as fly ash, blast furnace slags or mining residues. Although to date their principal applications have been as alternatives to Portland cement building materials, their properties make them suitable for a number of more advanced applications, including as photocatalytic nanocomposites for removal of hazardous pollutants from waste water or the atmosphere. For this purpose, they can be combined with photocatalytic moieties such as metal oxides with suitable bandgaps to couple with UV or visible radiation, or with carbon nanotubes or graphene. In these composites the geopolymers act as supports for the photoactive components, but geopolymers formed from wastes containing oxides such as Fe_2O_3 show intrinsic photoactive behaviour. This review discusses the structure and formation chemistry of geopolymers and the principles required for their utilisation as photocatalysts. The literature on existing photocatalytic geopolymers is reviewed, suggesting that these materials have a promising potential as inexpensive, efficient and ecologically-friendly candidates for the remediation of toxic environmental pollutants and would repay further development.

Keywords: geopolymers; photocatalysis; nanoparticles; degradation efficiency; TiO_2; Cu_2O; carbon nanotubes; graphene

1. Introduction.

The development of materials to mitigate the effects of global warming and pollution generated by human activities is becoming a matter of increasing urgency. The ecological problems to which solutions are being sought are the increase in greenhouse gas emissions arising from the manufacture of Ordinary Portland Cement (OPC) and electricity generation by coal-fired power plants, especially in developing nations with increased demands for infrastructure. Ecologically-friendly alternatives to OPC which do not involve the high-temperature reaction of clay and limestone, generating large amounts of CO_2 are inorganic polymers, otherwise known as geopolymers [1]. A further advantage of these materials over OPC is that they can be produced at temperatures from ambient to 80^{o}C by alkali activation of a range of aluminosilicate minerals [2-7]. For this reason, to date the major interest in geopolymers has been as alternatives to OPC, although they have many other high-

Preprints (www.preprints.org) | NOT PEER-REVIEWED | Posted: 13 September 2020 doi:10.20944/preprints202009.0296.v1

technology applications [8]. One such area of increasing interest is the mitigation of global environmental pollution problems, particularly air and water pollution. Over the past two or three decades photocatalytic degradation of environmental pollutants by exploiting the conversion of solar to chemical energy has attracted considerable attention. Heterogeneous photocatalysts have many advantages over other photocatalysts, since they can be cost-effective, stable, non-toxic, strongly oxidsing and effective at ambient temperature and pressure [9]. The combination of photocatalysts with geopolymers has been exploited in the construction industry to develop self-cleaning coatings for buildings, where the key factors are the aesthetic appearance and reasonable costs of cleaning maintenance [10]. Since geopolymers are environmentally friendly and can readily incorporate photocatalytically active materials such as ZnO, TiO_2, CuO and Fe_2O_3, they are an excellent option for construction applications. Geopolymers incorporated with photoactive materials in the presence of UV and UV-visible radiation [11] can oxidize and decompose the surface pollutants on a building or roadway, allowing the products to be subsequently easily removed later by rain, cleaning or washing with water because of the hydrophilic surface of the photocatalytic geopolymer with a low contact angle for water, allowing it to slide off [12-14] (Figure 1).

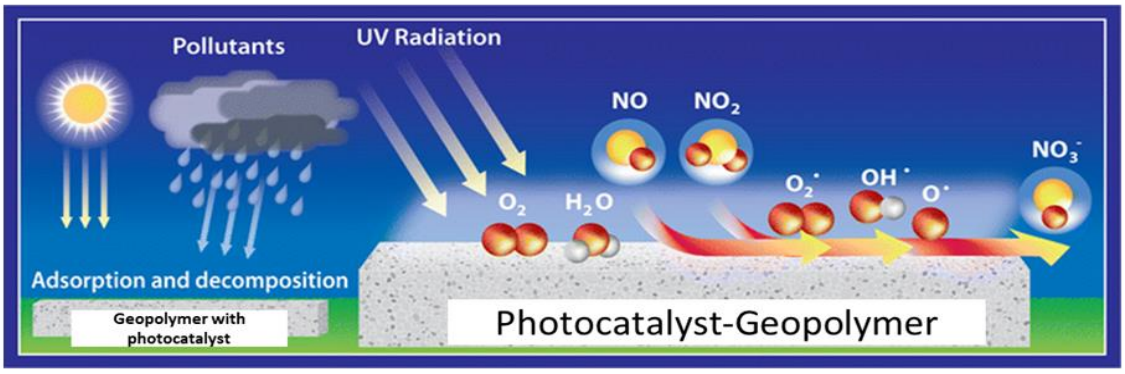

Figure 1. Schematic mechanism of a photocatalytic air-purifying geopolymer-based pavement, adapted from Boonen *et al.* [15]

A further ecological problem is associated with atmospheric pollution of waterways and the atmosphere resulting from manufacturing operations. A less well-researched but equally important environmental application of geopolymers has been as materials for the destruction of hazardous organic species in the atmosphere and in waterways. For this purpose, various photocatalytic species can be introduced into the geopolymer by exploiting its structure and chemistry, and the photocatalytic process can also be facilitated by the ability of the geopolymer to adsorb and immobilise the hazardous material in its structure. Thus, the combination of photocatalytic functionality with the environmental friendliness of

 doi:10.20944/preprints202009.0296.v1

geopolymers makes these potentially important materials for mitigation of climate change problems.

The present review outlines the important aspects of the synthesis and chemistry of aluminosilicate geopolymers, methods for the introduction of photocatalytic functionality by exploiting aspects of their structure and the application of these photocatalysts for the remediation of ecological problems.

2. Aluminosilicate geopolymers: composition, synthesis and structure

Aluminosilicate geopolymers are a class of alkali-activated materials, which, although having been known for many years, were first developed in their present form by Davidovits [1] by the action of alkali on dehydroxylated kaolin clay (metakaolin). These materials had the advantage of attaining strength at ambient or slightly elevated temperature and did not rely on the presence of crystalline phases for strength development. Davidovits also coined the name geopolymer by which these materials are now generally known. Alkali activation of other aluminosilicates such as coal fly ash [5] and ground blast furnace slag [7] was soon found to produce aluminosilicate geopolymers with comparable or superior mechanical properties and these are now most commonly used as construction or engineering materials. However, although thermally pre-treated kaolin minerals are still the most commonly used aluminosilicate source for specialised applications such as photocatalytic geopolymers, these minerals are commercially valuable, and the use of industrial wastes such as fly ash from coal-fired boilers for specialised geopolymer applications is attracting increasing attention.

Several synthetic methods for aluminosilicate geopolymers have been reported [8], but the most widely used is the reaction of a finely divided aluminosilicate source mineral or industrial waste material with an alkali metal hydroxide or a mixture of an alkali metal silicate and hydroxide. The setting characteristics of the resulting mixture can be controlled by adjusting the molar composition of the component oxides; in the case of metakaolin precursors, a molar composition of SiO_2/Al_2O_3~ 3, M_2O/SiO_2~ 0.3 and H_2O/M_2O~ 10 is reported [2] to set well and give a product with good strength, but these ratios can vary quite widely. The resulting geopolymer mixture is cured and hardened at temperatures between ambient and <100^{o}C. The mechanism of geopolymer formation involves the formation of aluminate and silicate monomers by alkali attack on the solid aluminosilicate starting material; these units then condense to a metastable gel which then becomes more fully cross-linked, allowing it to set and harden [16]. Some of these reaction steps may be concurrent and overlap, and their kinetics can depend on the nature of the starting material and the activating solution [16]. The steps of geopolymer synthesis are shown in Figure 2.

Preprints (www.preprints.org) | NOT PEER-REVIEWED | Posted: 13 September 2020 doi:10.20944/preprints202009.0296.v1

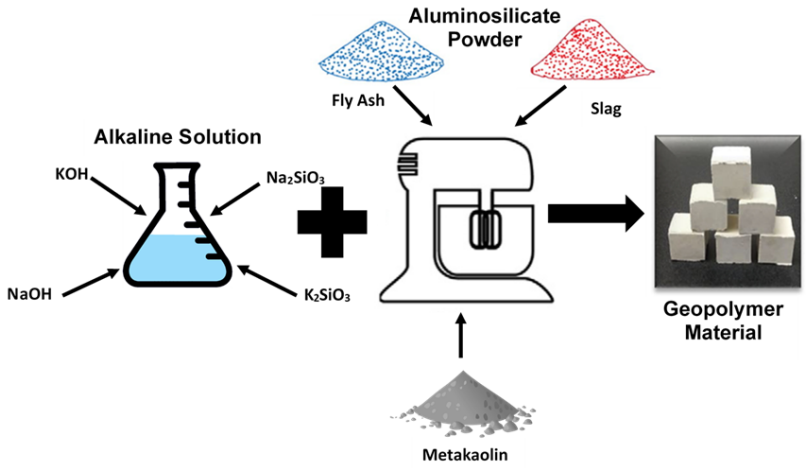

Figure 2. Schematic representation of the geopolymer synthesis procedure.

Aluminosilicate geopolymers consist of a random three-dimensional array of tetrahedral aluminate and silicate units joined through their apical oxygens. Their lack of long-range crystallographic order is reflected in their characteristic broad X-ray diffraction pattern similar to that of a glass [2]. The fourfold-coordinated aluminium atoms in this structure have been shown by ^{27}Al solid-state MAS NMR spectroscopy to be formed during the alkaline reaction by conversion of Al(VI) and Al(V) of the precursor to Al(IV) [17,18], resulting in a negative charge on each Al which is balanced by a positively-charged ion such as hydrated Na^+ or K^+ located in the interstices of the gel structure [2] (Figure 3). Since these charge-balancing ions are exchangeable, as in zeolites [19], they provide an important mechanism for manipulating the properties of the geopolymer and, in particular, they can be exploited to allow the introduction of photocatalytic moieties.

Preprints (www.preprints.org) | NOT PEER-REVIEWED | Posted: 13 September 2020 doi:10.20944/preprints202009.0296.v1

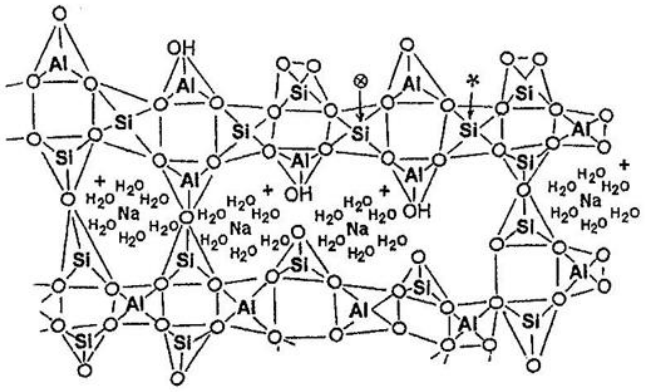

Figure 3. Proposed semi-schematic structure for a Na-geopolymer, adapted from Barbosa *et al*. [2].

3. Mechanism of photocatalysis in geopolymers

The photocatalysis mechanism in geopolymers is most usually extrinsic, i.e. it depends on the presence of an introduced semiconducting species such as ZnO or CuO. The action of light quanta on the semiconductor promotes a photoelectron from the filled valence band to the vacant conduction band, provided the energy of the photon is greater than or equal to the bandgap of the semiconductor. In the presence of water, the resulting photogenerated pair of the hole in the valence band and the electron in the conduction band can then react to produce $HO^{\bullet}$ radicals which are extremely powerful oxidising agents able to attack and destroy organic pollutants in solution. Concurrently, the holes in the valence band can react with oxygen to form anionic superoxide radicals, O_2^- . These species are not only oxidising agents in their own right but are able to prevent electron-hole recombination and maintain electron neutrality in the photocatalyst. Protonation of the superoxide radical forms the hyperoxyl radical, $HO_2^{\bullet}$, two of which can either combine to form $H_2O_2 + O_2$, or two highly reactive hydroxyl radicals $OH^{\bullet}$. All these oxidising species are highly reactive to organic compounds, reducing them to the benign products H_2O and CO_2. These processes are shown schematically in Figure 4.

Preprints (www.preprints.org) | NOT PEER-REVIEWED | Posted: 13 September 2020 doi:10.20944/preprints202009.0296.v1

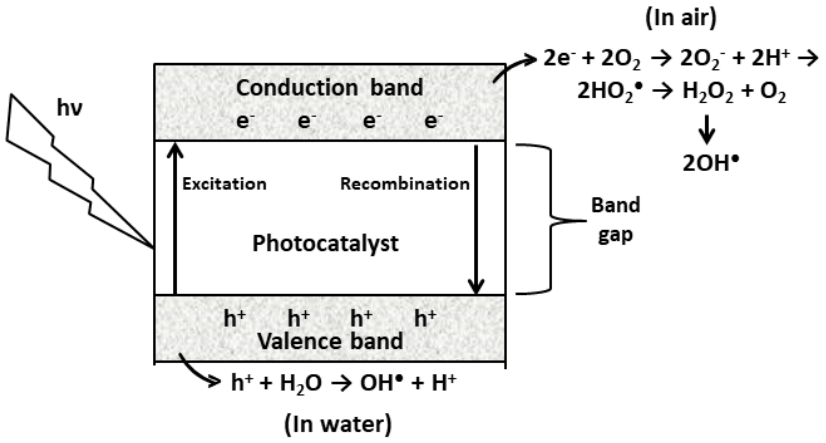

Figure 4. Schematic illustration of the photoactivation of a photocatalyst in water and air.

In greater detail, the photocatalytic process can be divided into four steps, namely:
(i) photogeneration of hole/electron pairs by UV irradiation, promoting the photoelectron from the valence band of the semiconductor to the empty conduction band. This produces a positively-charged hole in the valence band (h^+VB) and an electron in the conduction band (e^-(CB) (Eq. 1).

$$\text{Photocatalyst} + h\nu\,(UV) \rightarrow e^-(CB) + h^+(VB) \qquad (1)$$

(ii) separation of hole/electron pairs and their diffusion to the surface of the electrode. In the presence of adsorbed water the positive holes in the valence band produce hydroxyl radicals (Eq. 2).

$$H_2O(ads) + h^+(VB) \rightarrow OH^\bullet(ads) + H^+(ads) \qquad (2)$$

These $OH^\bullet$ radicals generated on the surface of the irradiated semiconductor are powerful oxidizing agents, able to attack adsorbed organic pollutants and destroy microorganisms.

(iii) oxygen ion sorption. Reaction of atmospheric oxygen with the electron promoted to the conduction band generates the anionic superoxide radical ($O_2^{-\bullet}$) (Eq. 3).

$$O_2 + e^-(CB) \rightarrow O_2^{-\bullet}(ads) \qquad (3)$$

The superoxide radical can take part in further oxidation processes and also plays a useful role in preventing electron-hole recombination.

Preprints (www.preprints.org) | NOT PEER-REVIEWED | Posted: 13 September 2020 doi:10.20944/preprints202009.0296.v1

(iv) photo-oxidation and photo-reduction reactions on the surface of the active catalytic sites. Protonation of the superoxide radical $O_2^{-\bullet}$ produces hydroperoxyl radicals ($HO_2^{\bullet}$) (Eq. 4), followed by the formation of H_2O_2 (Eq. 5) and its separation into highly reactive hydroxyl radicals ($OH^{\bullet}$) (Eq. 6). The oxidation and reduction processes both occur on the surface of the photoexcited semiconductor photocatalyst. The complete process is shown in Eqs. (4) to (6):

$$O_2^{-\bullet}(ads) + H^+ \rightarrow HOO^{\bullet}(ads) \quad (4)$$

$$2HOO^{\bullet}(ads) \rightarrow H_2O_2(ads) + O_2 \quad (5)$$

$$H_2O_2(ads) \rightarrow 2OH^{\bullet}(ads) \quad (6)$$

In the specific case where the photoactive semiconductor interacts with and destroys organic pollutants, the mechanism involves excitation of the organic pollutants by a photon of visible light ($\lambda > 400$ nm) from the ground state (Pollutants) to the triplet excited state (Pollutants *) (Eq. 7). The triplet excited state pollutant injects an electron into the conduction band of the photocatalyst and is then converted into a semi-oxidized radial cation ($Pollutants^{+}$) (Eq. 8) with the formation of superoxide radical anions (O_2-•) and hydroxyl radicals ($OH^{\bullet}$) . These $OH^{\bullet}$ radicals are mainly responsible for the oxidation of the pollutants (Eq. 9), but the positive holes photogenerated in the valence band and the photogenerated electrons in the conduction band are also responsible for oxidation and reduction of organic pollutants respectively (Eqs. 10 and 11) [20-23].

$$Pollutants + h\nu \rightarrow Pollutants^{*} \quad (7)$$

$$Pollutants^{*} + Photocatalyst \rightarrow Pollutants^{+} + Photocatalyst^{-} \quad (8)$$

$$Pollutants^{*} + OH^{\bullet}(ads) \rightarrow CO_2 + H_2O \text{ (via intermediates)} \quad (9)$$

$$Pollutants + H^{+}(VB) \rightarrow Oxidation\ products \quad (10)$$

$$Pollutants + e^{-}(CB) \rightarrow Reduction\ products \quad (11)$$

Thus, photocatalytic efficiency depends both on the ability of the photocatalyst to produce holes and electrons and on the creation of reactive free radicals. Therefore the specific surface area (SSA), morphology and bandgap of the photocatalyst are important properties which affect its efficiency. The bandgap is the distance between the valence band and the conduction band, and semiconductors, including SnO_2, MoO_3, ZnO, ZnS, Fe_2O_3, WO_3, CeO_2, CdS, ZrO_2, SnO_2, Cu_2O, and TiO_2, are commonly used as photocatalysts because of their unique electronic structure (occupied valence band and unoccupied conduction band) and sufficiently small bandgaps for solar excitation of an electron into the conduction band [24,25]. Ideally, a photocalyic semiconductor for insertion into a geopolymer matrix should be capable of efficiently utilizing visible or near-UV radiation (λ >400 nm), it should be biologically and chemically inert, photostable, inexpensive and non-toxic [26]. One oxide commonly used for this purpose is n-type TiO_2, but its bandgap of 3.03 eV is such that in normal sunlight only about 5% of the incident radiation is of suitable wavelength to photoexcite TiO_2 [27]. Another photoactive semiconductor is p-type Cu_2O, with a bandgap of 2.172 eV which couples well with visible radiation ($\lambda \leq 600$nm) [28]. The bandgaps of these

Preprints (www.preprints.org) | NOT PEER-REVIEWED | Posted: 13 September 2020 doi:10.20944/preprints202009.0296.v1

and other potential photoactive materials are listed in Table 1, and photoactive geopolymers containing some of these materials are the subject of this review.

Table 1. Band gap energy of various photocatalysts [29]

Photocatalyst	Bandgap (eV)	Photocatalyst	Bandgap (eV)
Diamond	5.4	SnO_2	3.8
Cubic ZnS	3.6	$SrTiO_3$	3.4
ZnO	3.3	TiO_2 (anatase)	3.2
α-Fe_2O_3	3.1	TiO_2 (rutile)	3.0
WO_3	2.8	CdS	2.4
Fe_2O_3	2.2	Cu_2O	2.1
CdSe	1.7	CdTe	1.4
WSe_2	1.2	Si	1.1

4. Aluminosilicate geopolymers with photocatalytic functionality

4.1. Geopolymer/TiO_2 photocatalysts.

TiO_2 is one of the more widely-used photocatalysts for environmental applications such as water purification, air cleaning and self-cleaning surfaces because of its good photocatalytic activity, chemical stability, low cost, long-term stability, ready availability and lack of toxicity [30–32]. One of the most challenging criteria for a suitable photocatalyst is that it must not rapidly recombine photogenerated electrons and holes. In the case of TiO_2 its photocatalytic efficiency can be increased by incorporating it into a TiO_2-based composite, thereby hindering its charge recombination [33]. In this way, TiO_2 has been immobilized by incorporation into a number of different construction materials, including window glass, cement-based materials, bricks, ceramics and geopolymers, producing environmentally friendly self-cleaning and air purification products [34].

Strini *et al.* [35] demonstrated the use of TiO_2-based photocatalytic geopolymers based on fly ash or metakaolin to decompose nitric oxide in air. The photocatalyst geopolymer was produced simply by mixing the geopolymer composition with P25 (a commercial mixture of rutile and anatase polymorphs of TiO_2). The ideal amount of TiO_2 was suggested to be 3 wt.% of the geopolymer paste, and the photocatalytic activity of the geopolymer composite depended on the type of binder and the curing conditions. The highest photocatalytic activity was found in a TiO_2/fly ash-based geopolymer composite cured at room temperature, which resulted in twice the NO degradation rate compared with that of a TiO_2/metakaolin geopolymer [35]. The photocatalytic activity was also found to depend on the curing parameters; curing at 60^oC produced a poorer photocatalyst, apparently due to segregation and depletion of the TiO_2 in the catalyst surface [35].

Bravo *et al.* [36] synthesised metakaolin-based geopolymer spheres with photocatalytic activity by coating TiO_2 nanoparticles on the surface of the spheres. These were produced by foaming an uncured geopolymer mixture with Polysorbate 80, then dropping the mixture from a syringe into polyethylene glycol at 80 ^oC, which reduces the surface tension and results in the formation of beads 2-3 mm in diameter. After drying at room temperature for 24 hr. then cured at 75 ^oC for 2 days, the beads were then coated with TiO_2 nanocrystals by heating them with TiO_2 at 1200 °C inside a quartz tube under high vacuum. SEM images confirmed the complete dispersion of TiO_2 within the geopolymer spheres. The

Preprints (www.preprints.org) | NOT PEER-REVIEWED | Posted: 13 September 2020 doi:10.20944/preprints202009.0296.v1

photocatalytic activity of the TiO_2/geopolymer spheres in the degradation of methylene blue dye showed 90% degradation after 10 hr. ultraviolet irradiation, compared with 4.5% degradation on the uncoated geopolymer spheres [36].

In another study, Chen *et al.* [34] deposited TiO_2 films by a sol-gel dip-coating method on a geopolymer substrate based on 95% fly ash and 5% metakaolin cured at room temperature. The geopolymer matrix was then dip-coated in a mixture of butyl titanate in ethanol with the addition of diethanolamine to increase the stability of the sol [34, 37]. The dip-coated samples were then annealed at 500, 600, 700 and 800 °C for 1 hr. and showed desirable photocatalytic properties for the degradation of methylene blue dye [34], especially the sample annealed at 600°C (Figure 5c), which was shown to contain the anatase phase of TiO_2 and a mesoporous morphology (Figure 5a,b). Improved photocatalytic activity of the composites could be obtained by double layer sol-gel coating, resulting in an increased specific surface area, but conversely, it may also increase the probability of electron-hole pair recombination and decrease the photocatalytic performance. A further problem observed with the sol-gel coating technique was a tendency for the films to crack upon drying, but this could be offset by the addition of 6 wt% polyvinylpyrrolidine (PVP) [34].

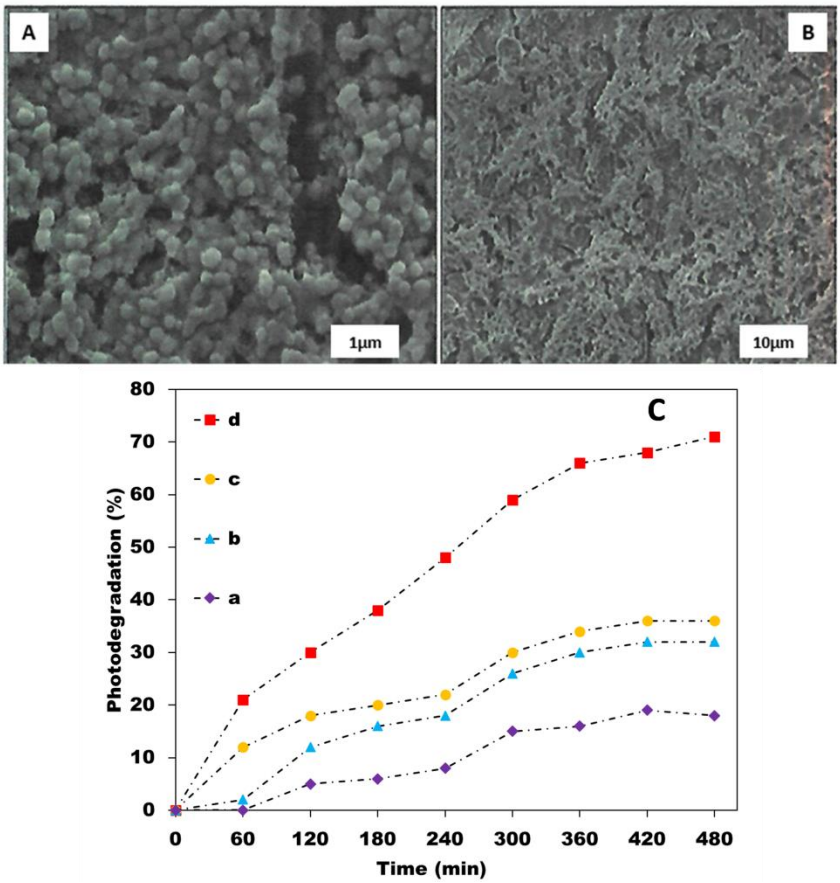

Figure 5. A. SEM images of a dip-coated TiO_2 film annealed at 600 °C for 1 hr, B. Surface morphology of a typical multilayer-coated TiO_2 film, C. Photocatalytic degradation of methylene blue by TiO_2 films coated on a geopolymer, annealed at (a) 500°C, (b) 800°C, (c) 700°C, (d) 600°C, from data of Chen *et al.* [34].

Gasca-Tirado *et al.*[38] reported an alternative method for incorporating photoactive TiO_2 into a metakaolin-based aluminosilicate inorganic polymer (geopolymer) by ion exchange

Preprints (www.preprints.org) | NOT PEER-REVIEWED | Posted: 13 September 2020 doi:10.20944/preprints202009.0296.v1

with ammonium titanyl oxalate monohydrate, $(NH_4)_2TiO(C_2O_4)_2.H_2O$. The efficiency of Ti incorporation was not improved by prior conversion of the geopolymer to the NH_4^+ form. This ion exchange method was found to facilitate the growth of anatase-type TiO_2 nanoparticles inside the geopolymer micropores, producing a photoactive geopolymer composite, demonstrated by its degradation of methylene blue (MB). The most efficient photoactivity was exhibited in a geopolymer cured at 90°C prior to ion exchange [38].

Yang *et al.* [39] studied the degradation of MB dye by foamed fly ash-based geopolymer-TiO_2 nanocomposites produced in two different ways. The use of a foamed geopolymer matrix increased its porosity, allowing the incorporation of a higher concentration of TiO_2 and improved contact with the dye solution. After alkali-activation, the fly ash geopolymer was foamed by the addition of oleic acid, followed by H_2O_2 then cured at 80 °C. Two methods were investigated for incorporating TiO_2 in the foamed geopolymer matrix; in one case the TiO_2 (P25) was directly mixed into the foamed geopolymer prior to curing, whereas in a second procedure, the cured foamed matrix was treated with a solution of TiO_2 in nitric acid, then calcined at 500 °C to crystallize the TiO_2 [39]. The most efficient photocatalytic degradation of MB dye was achieved in the composite containing 5 wt.% TiO_2 prepared by direct mixing, and was attained after 45 min of UV irradiation [39]. This suggests the potential of porous TiO_2/geopolymer composites for the treatment of industrially discharged wastewater. Table 2 compares the different synthesis methods and photodegradation applications of TiO_2/geopolymer photocatalysts.

Table 2. Comparison of the different TiO_2/geopolymer photocatalysts.

Adsorbent	Preparation Method	TiO_2 Type	TiO_2 Content	Adsorbate	Reference
TiO_2/fly ash or metakaolin geopolymer	Mixing	P25	3%	NO and NOx	Strini [35]
TiO_2/metakaolin geopolymer	Ion-Exchange	Anatase	28%	MB	Gasca-Tirado [38]
TiO_2/fly ash-metakaolin geopolymer	Sol-Gel dip coating	Anatase, Rutile	NA	MB	Chen [34]
TiO_2/fly ash geopolymer	Mixing	P25	10%	MB	Yang [39]
TiO_2/metakaolin geopolymer spheres	Inside quartz tube at high temperature	P25	10 mg	MB	Bravo [36]

4.2. Geopolymer/graphene photocatalysts

Graphene Oxide (GO) is a derivative of graphene, a 2-dimensional form of carbon that is attracting increasing interest as a functional material with useful properties such as high specific surface area, high electric conductance and good thermal conductivity. GO contains functional groups containing oxygen and can be synthesized by methods such as chemical oxidation or exfoliation of graphite [40] (Figure 6). The structure of GO is based on graphene and contains a number of oxygen functional groups (surface hydrophilic hydroxyl (-OH) and epoxy (C-O-C) groups and edge carboxyl (-COOH) groups). These groups allow GO to be dispersed in water and provide many active sites for linking to other functional groups and organic molecules [41]. GO has attracted attention for adsorption and catalytic applications; in particular, its photonic properties suggest its potential for enhancing the photocatalytic

Preprints (www.preprints.org) | NOT PEER-REVIEWED | Posted: 13 September 2020 doi:10.20944/preprints202009.0296.v1

properties of other materials. GO is typically suitable for the removal from water of organic dyes [42], antibiotics [43] and heavy metal ions [44].

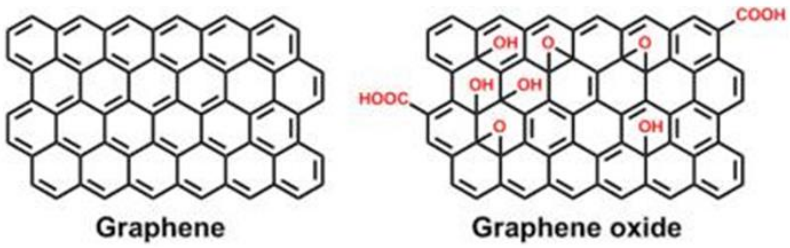

Figure 6. Structure of graphene and graphene oxide.

Lertcumfu *et al.* [40] studied the influence of GO additions on the photocatalytic properties of metakaolinite-based geopolymer composites and found that its addition can significantly improve the degradation of MB and Cr(VI) by comparison with pure geopolymer. The efficiency of the GO/geopolymer composite for the removal of MB and Cr(VI) was 93% and 65% respectively. These authors reported that the adsorption process followed the pseudo second-order kinetic model with an R^2 value > 98%. Moreover, these GO/geopolymer composites showed a potential application for waste water treatment owing to their photocatalytic activity with a low C/C_0 value of 0.6 after 2hr. of UV irradiation. Zhang *et al.* [45] reported the photoactivity of a nanocomposite synthesized by reaction of two-dimensional graphene with an alkali-activated granulated blast furnace slag (GBFS) geopolymer. This nanocomposite showed a high degree of methyl violet (MV) degradation under UV irradiation, especially in a composite containing 0.01 wt.% graphene, which had a degradation efficiency of 91.6 % after 110 min. of UV irradiation [45]. The degradation reaction of the MV dye followed a pseudo second-order kinetic model. Zhang *et al.* [46] reported the photocatalytic activity of a novel electroconductive graphene/fly ash-based geopolymer composite prepared by incorporation of 1 wt% of graphene into the alkali-activated geopolymer matrix prior to curing at room temperature. The addition of the graphene increased the electroconductivity of the composite by 348.8 times compared with that of the geopolymer without graphene, and the synergic effect of the graphene with the matrix red-shifted the maximum absorption wavelength of the composite into the visible region [46]. Furthermore, the presence of the graphene was shown by nitrogen adsorption-desorption isotherms to effectively improve the pore structure of the composite. The photoactive composite was found to degrade indigo carmine (IG) dye with an efficiency of 90.2%, three time greater than the photocatalytic efficiency of the geopolymer matrix without

Preprints (www.preprints.org) | NOT PEER-REVIEWED | Posted: 13 September 2020 doi:10.20944/preprints202009.0296.v1

graphene, and this catalytic performance for the removal of organic pollutants was unchanged after 5 cycling runs of UV irradiation [46]. Furthermore, the graphene structure was shown to be unchanged after the dye photodegradation cycles. The proposed mechanism involves interaction of the graphene with Fe_2O_3 particles from the fly ash geopolymer matrix in which the photogenerated electrons from the former are rapidly transfered to the π-conjugated system of the graphene, efficiently separating the photogenerated electron-hole pairs and allowing them to oxidize the H_2O molecules adsorbed on the iron oxide surfaces. The resulting hydroxyl radicals which oxidize and degrade the dye molecules adsorbed on the iron oxide surfaces [46]. In experiments to shed further light on this mechanism, it was found that the addition of benzoquinone, which traps hydroxyl radicals, reduced the dye degradation efficiency from 91.6% to 70.8%, whereas the addition of tertiary butyl alcohol, which traps superoxide radicals, reduced the degradation efficiency to 35.1% (Figure 7). These experiments suggest that graphene, can act as an electron acceptor to enhance the oxidation degradation capacity of geopolymers.

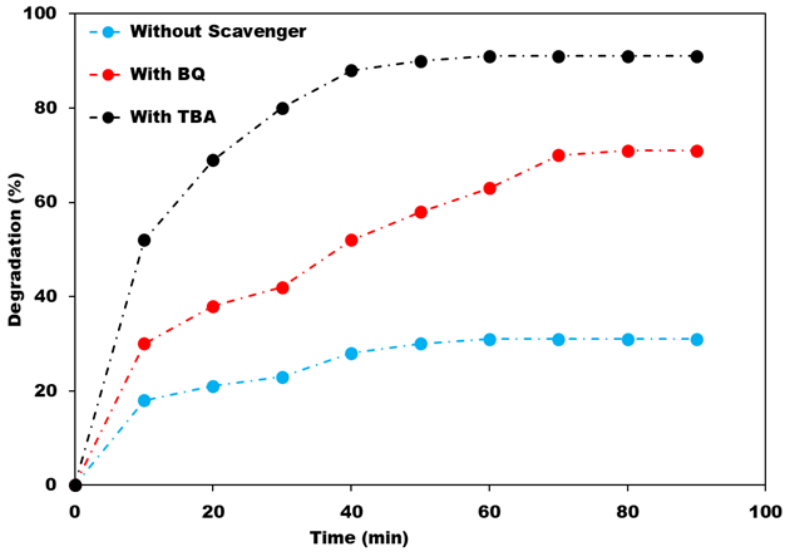

Figure 7. The effect of tertiary butyl alcohol (TBA) and benzoquinone (BQ) radical scavengers on the photocatalytic degradation of indigo carmine, data taken from Zhang *et al*. [46].

Table 3, which summarises the reported investigations of photoactive geopolymers containing graphene or graphene oxide, highlights the varying experimental conditions used by different researchers, making a direct comparison of the photocatalytic results impossible. Although the available research data on these graphene/geopolymer photocomposites are very promising, considerably more theoretical and experimental research is required on these systems.

Preprints (www.preprints.org) | NOT PEER-REVIEWED | Posted: 13 September 2020 doi:10.20944/preprints202009.0296.v1

Table 3. Summary of the different studies on graphene and graphene oxide geopolymer photocatalysts.

Matrix	Preparation method	Graphene content (%)	Adsorbate	Reference
graphene/fly ash-based geopolymer	Mixing	0.1, 0.4, 0.7 and 1	Indigo carmine	Zhang [47]
graphene oxide/calcined kaolinite-based geopolymer	Mixing	0, 2.5, 5, and 10	Methylene blue	Rujijanagul [40]
graphene/blast furnace slag-based geopolymer	Mixing	0.01	Methyl violet	Zhang 2016 [45]

4.3. Geopolymer/Cu_2O photocatalysts

Cu_2O, a prominent p-type semiconductor, acts as a photocatalyst under visible light irradiation (≤600 nm). Its direct bandgap energy of 2.2 eV is readily excited by wavelengths in the visible region, giving it a significant absorption coefficient (up to ~10^4 cm^{-1}) in this region. This suggests that Cu_2O should act as a stable photocatalyst for the photochemical decomposition of H_2O with the generation of O_2 and H_2 under visible light irradiation and that it should also be a suitable candidate for the photocatalytic degradation of organic pollutants under visible light irradiation. The photocatalytic possibilities of Cu_2O were investigated by Huang *et al* [48] who demonstrated its photodegradation of methyl orange, but reported that it was readily deactivated by photocorrosion, especially when in the form of nanoparticles [48]. An improvement in its catalytic performance was obtained with larger microparticles which underwent photocorrosion more slowly, and its performance was also improved by the addition of 0.1 mmol/L of methanol which acted as a hole scavenger [48]. The photocatalytic behaviour of the different well-formed crystal facets of Cu_2O microcrystals with well-formed facets was investigated by Zheng et al [47]. They observed that during the photodegradation of methyl orange, the {100} and {110} faces gradually transformed into the {111} facets of nanosheets which exhibit stable photocatalytic activity [47]. These results, and the low toxicity, low cost and environmental friendliness of Cu_2O suggest its use as a possible alternative to other common photocatalysts such as TiO_2 for the photocatalytic degradation of organic contaminants, particularly when combined with ecologically-friendly geopolymers. These considerations led Fallah et al [49] to investigate a novel photoactive inorganic polymer composite containing copper(I) oxide nanoparticles. The Cu_2O nanoparticles were synthesized by the solution precipitation method, producing cubic crystallites of nanometer size. Metakaolin-based Cu_2O/geopolymer composites were prepared by mixing 10-30 wt.% of pre-synthesized Cu_2O nanoparticles with the geopolymer paste and curing for 12 hr. at ambient temperature. The photocatalytic activity of the Cu_2O/geopolymer composite in the degradation of methylene blue (MB) was studied under the UV-irradiation [49]. Although the nano-Cu_2O itself did not adsorb the methylene blue dye, its incorporation of up to 20 wt. % into the geopolymer composites increased their adsorption ability due to adsorption within the pores of the geopolymer matrix. Under UV radiation, the composites removed the MB dye from solution by a combination of adsorption and photodegradation (Figure 8), without deterioration of the geopolymer structure or the photoactive Cu_2O component. This suggested that these geopolymer composites should function as useful new materials for the removal of organic pollutants from water or the

Preprints (www.preprints.org) | NOT PEER-REVIEWED | Posted: 13 September 2020 doi:10.20944/preprints202009.0296.v1

atmosphere. The degradation of the MB dye followed a pseudo-second order kinetic model [49].

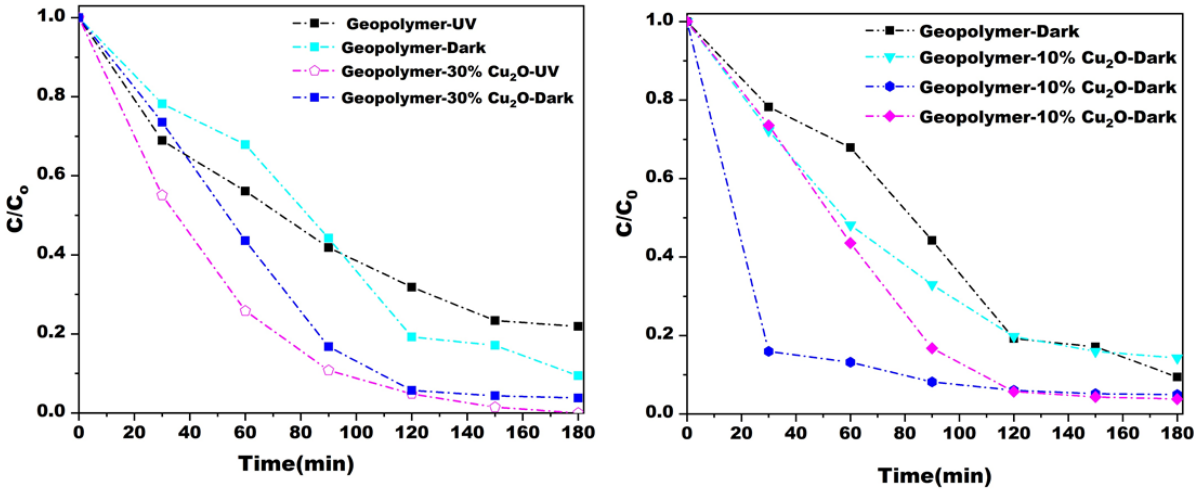

Figure 8. (a) Residual concentration (C/C_0) of methylene blue dye upon exposure to the geopolymer matrix (GP) and the Cu_2O-geopolymer composites versus time in the dark, (b) comparison of the degradation of methylene blue dye by the geopolymer matrix and the 30 wt% Cu_2O-geopolymer composite in the dark and under UV illumination. Data from Falah *et al* [49].

4.4 Geopolymer/carbon nanotube photocatalysts

Carbon nanotubes (CNTs), are graphite sheets rolled up into cylinders with partly one-dimensional nanostructures. CNTs have diameters of a few nanometers and lengths of some millimeters. CNTs can occur as single-walled nanotubes (SWCNTs), double-walled nanotubes (DWCNTs) and the multi-walled nanotubes (MWCNTs), the latter consisting of multiple layers of graphite arranged in concentric cylinders [50]. CNTs have been successfully used as catalyst supporting materials with properties superior to those of other regular catalyst supports. CNTs have large specific surface areas and have excellent capability for absorbing toxic materials such as nitrogen oxides and polluted waste water [51,52]. They are also useful for reinforcing geopolymers. Bi *et al*. [53] synthesised metakaolin-based geopolymer nanocomposites containing CNTs by ultrasonically dispersing 0.1, 0.25, and 0.5 vol % of CNTs into a mixture of NaOH and sodium silicate solution, followed by blending with metakaolin powder, curing at 40°C for 2 hr. and aging at 60°C for 24 hr. Before use, the CNTs were given a surface silica coating by treatment with a mixture of H_2SO_4 and HNO_3, followed by a mixture of TEOS and NH_4OH. The resulting good distribution of the CNTs in the geopolymer matrix and the interfacial interaction between the SiO_2 coating and the geopolymer matrix (Figure 9) were found significantly to improve the mechanical properties of the geopolymer nanocomposites [53] and suggested their application as a self-sensing structural material with ultrahigh sensitivity. Although the possible use of these composites as photoactive materials has not yet been investigated, the photoactive properties of the closely-related graphene/geopolymer composites (Section 4.2) suggests investigation of the CNT/geopolymer composites would be worthwhile.

Preprints (www.preprints.org) | NOT PEER-REVIEWED | Posted: 13 September 2020 doi:10.20944/preprints202009.0296.v1

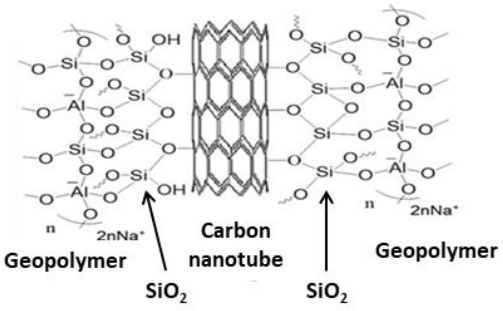

Figure 9. Schematic representation of the interface between a SiO_2-treated carbon nanotube surface and a geopolymer matrix.

4.5. Other geopolymer photocatalysts

Following their previous promising results using Cu_2O for the photocatalytic degradation of methyl orange [48], Huang *et al*. [54] obtained an improved photocatalytst by combining TiO_2 with Cu_2O. Their Cu_2O/TiO_2 heterostructures, prepared by an alcohol-aqueous based chemical precipitation method, showed greatly improved photocatalytic activity compared with pure TiO_2 (P25), especially 50:50 Cu_2O/TiO_2 compositions [54]. The photocatalytic efficiency of these for the degradation of acid orange II dye were reported to be 6 times greater than pure TiO_2 under UV-visible light, and 27 times greater under visible light [54]. Based on these findings, Falah *et al*. [55] prepared novel photoactive composites of spherical Cu_2O-TiO_2 nanoparticles with aluminosilicate geopolymers which would act both as an adsorbent and photocatalyst. The synthesis procedure of the Cu_2O-TiO_2 nanoparticles from copper acetate and TiO_2 (P25) is shown schematically in Figure 10. After SEM characterization of the heterostructured nanoparticles, 10-30 wt.% were added to an uncured metakaolin-based geopolymer mixture and cured at room temperature [55]. Under dark conditions, the geopolymer photocatalyst was found adsorb methylene blue dye, following first-order kinetics and Freundlich-type isotherms, but the adsorption process was less efficient in geopolymer composites containing 10 wt.% of Cu_2O/TiO_2 than in the geopolymer matrix alone, probably due to blocking of the adsorption sites by the oxide nanoparticles. Under UV irradiation, the Cu_2O/TiO_2 geopolymer composite removed the methylene blue dye by a combination of adsorption and photodegradation without destroying the geopolymer structure

Preprints (www.preprints.org) | NOT PEER-REVIEWED | Posted: 13 September 2020 doi:10.20944/preprints202009.0296.v1

[55], suggesting that these new geopolymer composites should be suitable for efficiently removing organic pollutants from water or the atmosphere.

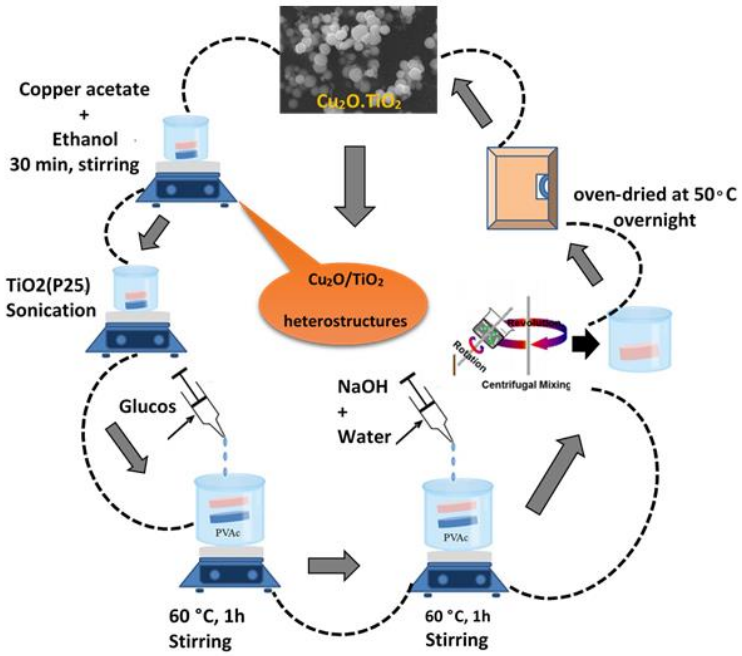

Figure 10. Schematic diagram of the synthesis of Cu_2O/TiO_2 nanoparticles by an alcohol/aqueous- based chemical precipitation method.

The previous study by Falah *et al*. [55] of Cu_2O/TiO_2 geopolymer photocatalysts indicated that these materials can play a dual adsorption-photoactive role, but the presence of the nanoparticle oxides can hinder adsorption by blocking the pores in the geopolymer matrix. This led Falah *et al*. [56] to modify the matrix by inserting a large tertiary ammonium ion, cetyltrimethylamonium bromide, (CTAB) to facilitate access of the Cu_2O/TiO_2 nanoparticles into the geopolymer pores. The amount of CTAB, based on the cation exchange capacity of the starting clay, was added, together with Cu_2O/TiO_2 nanospheres prepared as in [55], to a metakaolin-based geopolymer composition prior to curing at 40 ^oC. In experiments to remove methylene blue by a combination of adsorption and photodegradation processes, the adsorption of the dye by the CTAB-modified Cu_2O/TiO_2-geopolymer followed pseudo second-order kinetics and Freundlich-Langmuir type isotherms. A comparison of the photocatalytic behavior of CTAB-modified Cu_2O/TiO_2-geopolymer composites and Cu_2O/TiO_2-geopolymer composites without CTAB under UV-illumination (Figure 11) shows that CTAB-modification of the Cu_2O/TiO_2-geopolymer containing 10 wt. % of Cu_2O/TiO_2 nanoparticles results in an improvement in the removal of methylene blue from 55% in the unmodified composite to 97% in the CTAB-modified compound in 60 min. under UV irradiation, suggesting that further experiments to modify the geopolymer matrix may prove fruitful.

Preprints (www.preprints.org) | NOT PEER-REVIEWED | Posted: 13 September 2020 doi:10.20944/preprints202009.0296.v1

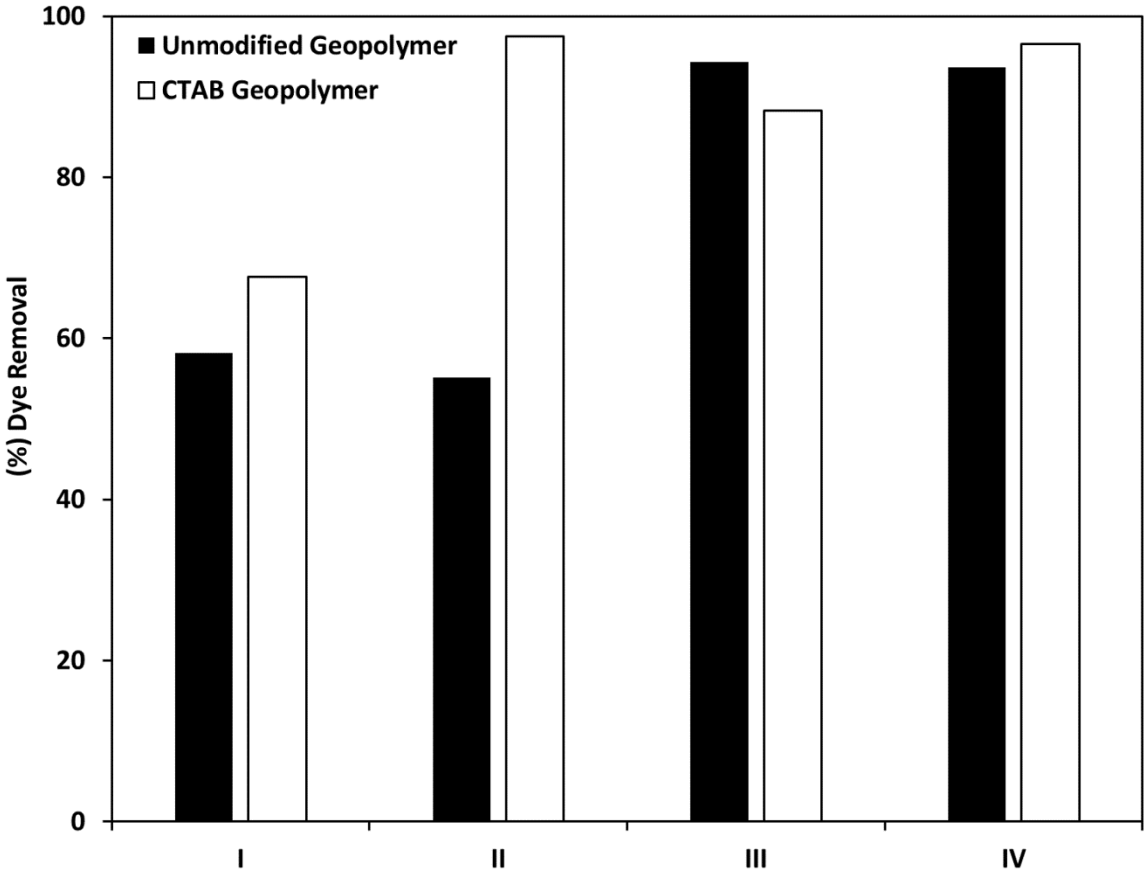

Figure 11. Removal of methylene blue dye from solution after 90 min. UV irradiation by composites based on CTAB-modified inorganic polymer matrices compared with geopolymers based on unmodified matrices. (I) geopolymer matrix, (II) 10wt.% Cu_2O/TiO_2-geopolmer, (III)10wt.%Cu_2O/geopolymer, (IV) 10wt%TiO_2/geopolymer. Data from Falah *et al*. [55,56].

Zailan *et al*. [57] studied the effect of ZnO nanoparticles on the photocatalytic degradation of methylene blue by F-class fly ash-based geopolymers under ultraviolet irradiation. ZnO nanoparticles (2.5-10 wt.%) were dry-mixed with the fly ash prior to activation with sodium silicate and sodium hydroxide. The ZnO/fly ash geopolymer composite showed satisfactorily efficient photocatalytic degradation of methylene blue after 150 min of exposure to sunlight, and by increasing the ZnO content, more active sites were produced on the photocatalyst surface, increasing the number of hydroxyl and superoxide radicals, thereby facilitating the photodegradation of the dye. The effect of ZnO-based geopolymer paste surfaces containing various amounts of ZnO on the photocatalytic degradation of methylene blue dye under UV light is shown in Figure 12.

Preprints (www.preprints.org) | NOT PEER-REVIEWED | Posted: 13 September 2020 doi:10.20944/preprints202009.0296.v1

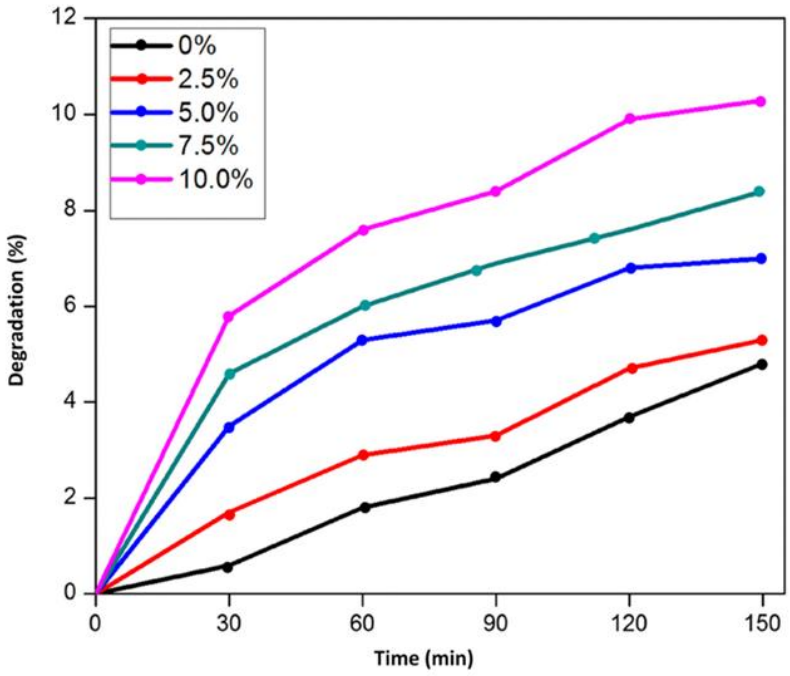

Figure 12. Degradation of methylene blue dye under UV irradiation by ZnO-based geopolymers containing different amounts of ZnO nanoparticles, re-drawn from data of Zailan *et al*. [57].

A novel photocatalytic geopolymer based on ground granular blast furnace slag (GGBFS) containing ZnO and graphene has been developed by Zhang *et al.* [58] for applications such as solar hydrogen production and treatment of wastewater polluted with dye. The photoactive geopolymer was prepared by mixing the slag with0.1 wt. % graphene, activating with NaOH solution and curing at 20°C under 90% relative humidity for 24 hr. This material was then ground and the charge-compensating Na^+ ions of the geopolymer exchanged with NH_4^+ by treatment with NH_4NO_3 solution, followed by the introduction of zinc from a solution of $Zn(CH_3COO)_2$. At low loadings, the ZnO was amorphous, but at higher Zn contents it was in the crystalline form of zincite. The photoactive geopolymer was dried at 65 °C and calcined at 400 °C for 4 h in a nitrogen atmosphere. The resulting combination of the ZnO, graphene and slag in a geopolymer of composition 15ZnO/GGBFS showed 92.7% degradation efficiency of basic violet 5BN dye in wastewater under UV irradiation, compared with degradation by the geopolymer matrix alone or ZnO alone (9.7% and 58.2% respectively, under the same conditions). The degradation efficiency of this geopolymer composite was also relatively unchanged over 5 reaction cycles (Table 4) and also showed excellent photocatalytic activity for the production of hydrogen (2281.3 μmol/g) from water (Fig. 13), compared with ZnO alone [58]. It was suggested that the slag-based geopolymer matrix acts as a support for the graphene and the photoactive ZnO semiconductor, which under irradiation produces photoinduced electrons in the conduction band. The proximity of the ZnO to the graphene enables the efficient transmission of these photoelectrons to the π-bond conjugate system of graphene, resulting in the efficient separation of photoinduced electron-

Preprints (www.preprints.org) | NOT PEER-REVIEWED | Posted: 13 September 2020 doi:10.20944/preprints202009.0296.v1

hole pairs, producing the hydroxyl radicals responsible for the second-order kinetic photodegradation of dye-polluted waste waters [58].

Table 4. Degradation efficiency of basic violet 5BN dye by a slag-based geopolymer containing 0.1 wt% graphene and 15ZnO under UV irradiation over five reaction cycles [58].

Cycle number	Degradation (%)
1	92.7
2	90.6
3	89.7
4	88.5
5	87.8

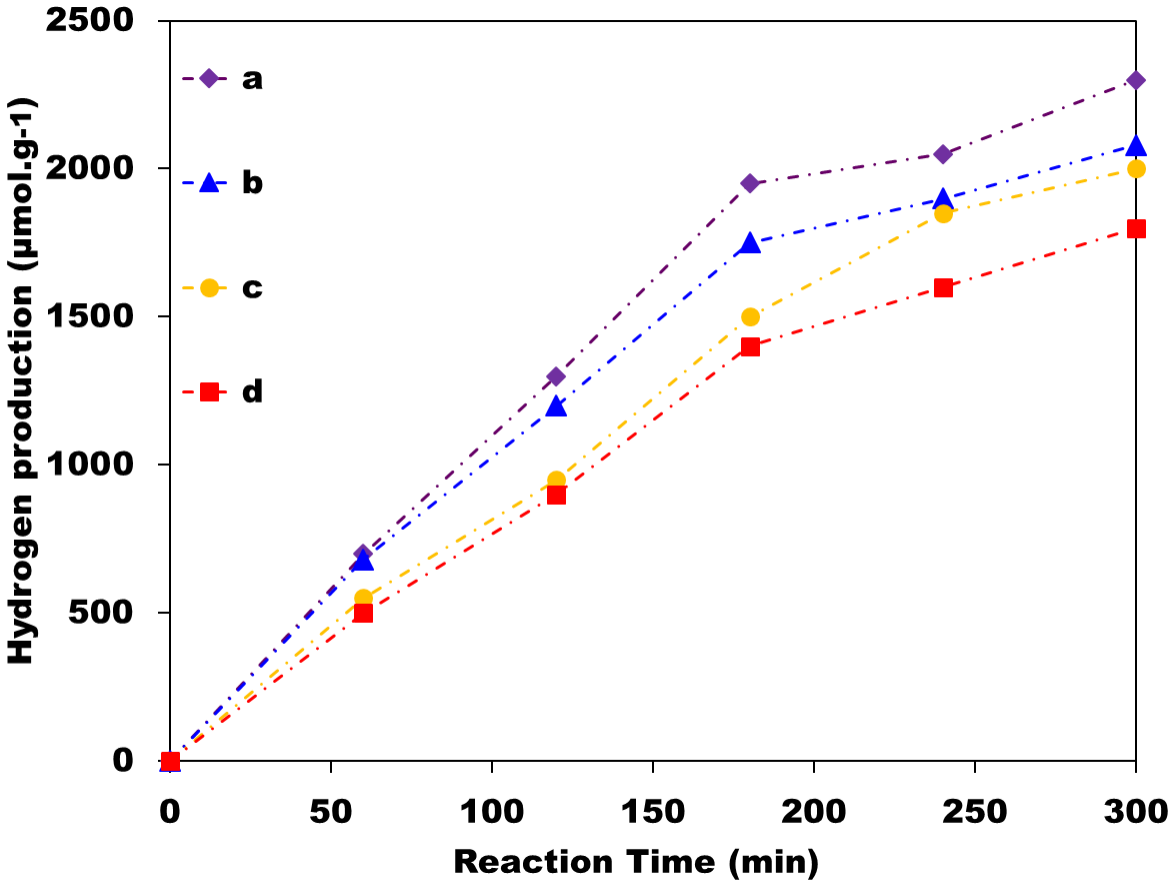

Figure 13. UV photocatalytic hydrogen production from water by ZnO/graphene GGBFS-based photocatalysts containing 0.01 wt% graphene, as a function of ZnO content. (a) 15ZnO, (b) 10ZnO, (c) 20ZnO, (d) 2ZnO. Data from Zhang *et al.* [58].

Zhang *et al* [59] have also reported the successful use of a GGBFS-based geopolymer containing graphene and CdO for the photodegradation of direct fast bordeaux dye in waste water. The preparation of the photoactive geopolymer was similar to that described above for the ZnO-graphene/GGBFs geopolymer composite [59], substituting a solution of $Cd(NO_3)_2.4H_2O$ for $Zn(CH_3COO)_2$ solution. Samples containing 1-16 wt.% CdO were investigated but the most efficient photodegradation of the dye under UV irradiation (close to 100% after 100 min.) was obtained with the photocatalyst containing 8 wt.% CdO (Figure 14).

Preprints (www.preprints.org) | NOT PEER-REVIEWED | Posted: 13 September 2020 doi:10.20944/preprints202009.0296.v1

By contrast with the results for the corresponding ZnO photocomposite [59], the dye photodegradation by the CdO photocomposite followed first order kinetics [59].

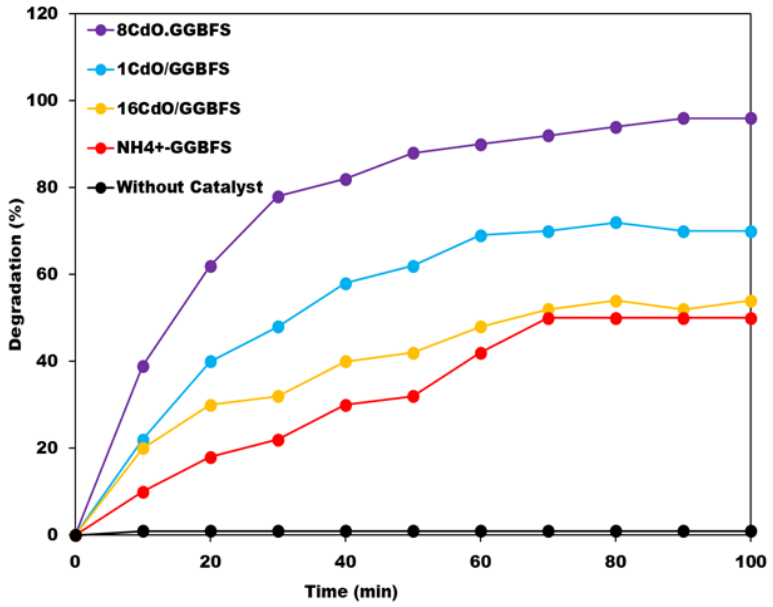

Figure 14. Photocatalytic degradation under UV irradiation of direct fast bordeaux dye by CdO/graphene GGBFS-based photocatalysts as a function of CdO content, compared with NH_4^+-exchanged GGBFS geopolymer, from data of Zhang *et al* [59].

Saufi *et al.* [60] have reported an interesting geopolymer with intrinsic photoactive properties prepared from the mineral perlite, an aluminosilicate mineral containing 74.8 wt.% SiO_2, 12.5 wt.% Al_2O_3, 4.5 wt.% Na_2O, 5.42 wt.% K_2O, 0.9 wt.% Fe_2O_3 and 0.7 wt.% CaO. After activation with NaOH and sodium silicate, the geopolymer was cured at 60 ^oC for 24 hr. The photocatalytic properties of this geopolymer, which were suggested to be associated with the Fe_2O_3 component of the perlite, were shown to degrade methylene blue dye under UV irradiation with 97.8% efficiency in 4 hr. with a second-order kinetic process (Figure 15) [60]. These results open up the prospect of new types of geopolymers in which the photoactive moiety is supplied by one of the components naturally occurring in the aluminosilicate precursor.

Preprints (www.preprints.org) | NOT PEER-REVIEWED | Posted: 13 September 2020 doi:10.20944/preprints202009.0296.v1

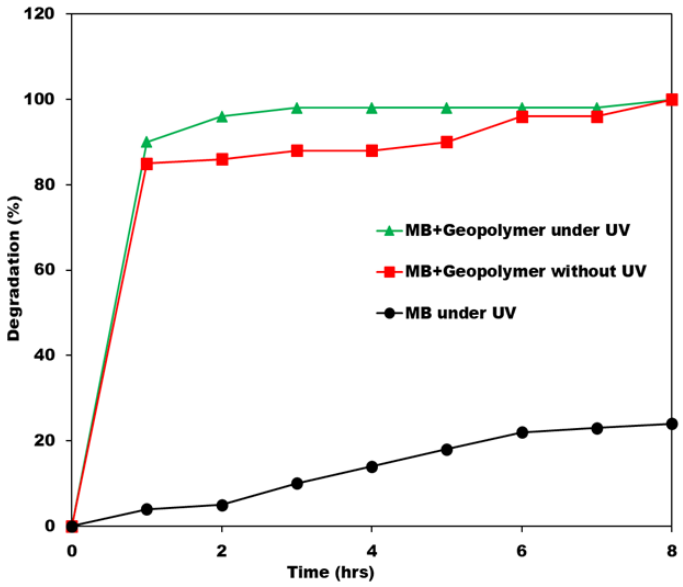

Figure 15. Photocatalytic degradation efficiency of methylene blue dye by perlite-based geopolymer in the dark and under UV radiation, from data of Saufi *et al.* [60].

A fly ash-based geopolymer with similar intrinsic photoactivity was reported by Zhang *et al* [61], in which the photoactive components were the 4.4% Fe_3O_3 and 1.1% TiO_2 in the starting material. This geopolymer was shown to remove methylene blue dye from solution under UV irradiation with 92.8% efficiency (Figure 16) by a combination of adsorption in the geopolymer pores following pseudo-second order kinetics, and photodegradation, following third-order kinetics [61].

Preprints (www.preprints.org) | NOT PEER-REVIEWED | Posted: 13 September 2020 doi:10.20944/preprints202009.0296.v1

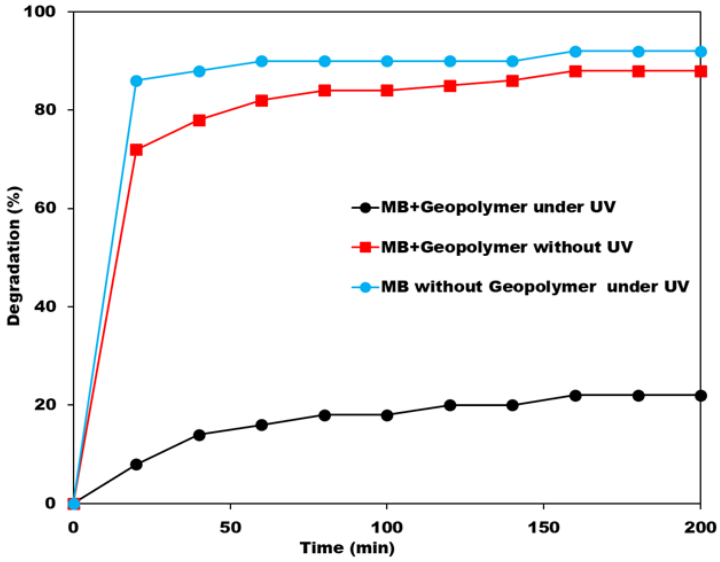

Figure 16. Photocatalytic degradation efficiency of methylene blue dye by fly ash-based geopolymer un the dark and under UV radiation, from data of Zhang *et al* [61].

He *et al* [62] reported an unusual photoactive electroconductive geopolymer prepared by alkali activation of silicomanganese slag waste. The slag was blended with carbon black, activated with NaOH, cured for 6 hr. at 80°C then powdered. The powder was converted to the NH_4^+ form by immersion in a solution of NH_4CH_3COO, washed and dried, then impregnated with a solution of $(NH_4)_6Mo_7O_{24}.4H_2O$ before calcining at 400°C for 4 hr. to produce a geopolymer containing $CaMoO_4$ and carbon black [62]. In addition to its electroconductive properties, the photocatalyst containing an optimum $CaMoO_4$ content of composition of photocatalyst was found to degrade BV5 dye, achieving close to 100% degradation under UV irradiation after 80 min.

5. Conclusions

Geopolymers have been shown to be capable of forming photocatalytic nanocomposites for removal of hazardous pollutants from waste water or the atmosphere. These ecologically-friendly inorganic materials can be produced at temperatures below 100°C from industrial wastes such as fly ash, blast furnace slags or mining residues, and their chemical and physical properties enable them to act as supports for photoactive species, including TiO_2, Cu_2O, Fe_2O_3, or carbon nanotubes and graphene. The combination of some of these species has been exploited in some cases to hinder electron/hole recombination, enhancing the performance of the photocatalyst. Geopolymers formed from industrial wastes such as fly ash or ground granulated blast furnace slag, or minerals such as perlite which contain photoactive Fe_2O_3 contaminants also display intrinsic photoactivity without the need for additional components; these materials have been less widely reported, but would be worth further investigation. In most cases the photocatalytic efficiency of these compounds was determined by their degradation of a dye such as methylene blue, both in the dark and under UV (solar) radiation.

These studies indicated a dual mechanism of adsorption by the geopolymer matrix and photodegradation by the photoactive species present. Thus, photoactive geopolymers represent promising ecologically-friendly, cost-effective and efficient materials for the remediation of toxic environmental pollutants.

References

1. Davidovits, J. Geopolymers: inorganic polymeric new materials, J. Therm. Anal. Calorim. **1991** *37* 1633–1656. https://doi.org/10.1007/BF01912193.
2 Barbosa, V.F.F.; MacKenzie, K.J.D.; Thaumaturgo, C. Synthesis and characterisation of materials based on inorganic polymers of alumina and silica: sodium polysialate polymers, Int. J. Inorg. Mater. 2000 *2* 309–317. https://doi.org/10.1016/S1466-6049(00)00041-6.

3. MacKenzie, K.J.D.; Komphanchai, S.; Vagana, R. Formation of inorganic polymers (geopolymers) from 2:1 layer lattice aluminosilicates. J. Eur. Ceram. Soc. **2008** *28* 177-81.
4. Lemounga, P.N.; MacKenzie, K.J.D.; Chinje Melo, C.F. Synthesis and thermal properties of inorganic polymers (geopolymers) for structural and refractory applications from volcanic ash. Ceram. Int. **2011** *37* 3011-8.
5. Xu, G.; Shi X. Characteristics and applications of fly ash as a sustainable construction material: A state-of-the-art review. Res., Cons. Recyc. **2018** *136* 95-109.
6. Temuujin, J.; Minjigmaa, A.; Bayarzul, U.; Kim, D.S.; Lee, S-H.; Lee, H.J.; Ruescher, C.; MacKenzie, K.J.D. Properties of geopolymer binders prepared from milled pond ash. Mater. de Constr. **2917** *67* e134.
7. Rashad, A.M. A comprehensive overview about the influence of different additives on the properties of alkali-activated slag- a guide for civil engineer. Constr. Build. Mater. **2013** *47* 29-55.
8. MacKenzie, K.J.D. Inorganic polymers (geopolymers). In: Encyclopedia of Polymer Science and Technology, Wiley **2017** pp. 1-31. DOI:10.1002/0471440264.pst165.pub2. ISBN 9780471440260.
9. Santhi, K.; Rani, C.; Karuppuchamy, S. Synthesis and characterization of a novel SnO/SnO_2 hybrid photocatalyst, J. Alloys Compd. **2016** *662* 102–107. doi:10.1016/j.jallcom.2015.12.007.
10. Boonen, E.; Beeldens, A. Photocatalytic roads: From lab tests to real scale applications, Eur. Transp. Res. Rev. **2013** *5* 79–89. doi:10.1007/s12544-012-0085-6.
11. Falah, M. Synthesis of New Composites of Inorganic Polymers (Geopolymers) with Metal Oxide Nanoparticles and their Photodegradation of Organic Pollutants, **2015** http://researcharchive.vuw.ac.nz/handle/10063/4847
12. Shen, S.; Kronawitter, C.; Kiriakidis, G. An overview of photocatalytic materials, J. Mater. **2017** *3* 1–2. doi:10.1016/j.jmat.2016.12.004.
13. Santhi, K.; Rani, C.; Karuppuchamy, S. Synthesis and characterization of a novel SnO/SnO_2 hybrid photocatalyst, J. Alloys Compd. **2016** *662* 102–107. doi:10.1016/j.jallcom.2015.12.007.
14. Karthikeyan, C.; Arunachalam, P.; Ramachandran, K.; Al-Mayouf, A.M.; Karuppuchamy, S. Recent advances in semiconductor metal oxides with enhanced methods for solar photocatalytic applications, J. Alloys Compd. **2020** *828* 154281. doi:10.1016/j.jallcom.2020.154281.
15 Boonen, E.; Beeldens, A. Recent Photocatalytic Applications for Air Purification in Belgium, Coatings. **2014** *4* 553–573. doi:10.3390/coatings4030553.
16. Provis, J.L.; van Deventer, J.S.J. Geopolymerisation kinetics. 2. Reaction kinetic modelling, Chem. Eng. Sci. **2007** *62* 2318–2329. https://doi.org/10.1016/j.ces.2007.01.028.

17. MacKenzie, K.J.D. and Smith, M.E. Multinuclear Solid State NMR of Inorganic Materials, Pergamon Materials Series Vol. 6, Pergamon/Elsevier, Oxford, **2002**, p. 304.
18. Rowles, M.R.; Hanna, J.V.; Pike, K.J.; Smith, M.E.; O'Connor, B.H. ^{29}Si, ^{27}Al, ^{1}H and ^{23}Na MAS study of the bonding character in aluminosilicate inorganic polymers. Appl. Magn. Reson. **2007** *32* 663-89.
19. O'Connor, S.J.; MacKenzie, K.J.D.; Smith, M.E.; Hanna, J.V. Ion exchange in the charge-balancing sites of aluminosilicate inorganic polymers. J. Mater. Chem. **2010** *20* 10234-40.
20. Malathi, A.; Madhavan, J.; Ashokkumar, M.; Arunachalam, P. A review on $BiVO_4$ photocatalyst: Activity enhancement methods for solar photocatalytic applications, Appl. Catal. A Gen. **2018** *555* 47–74. doi:10.1016/j.apcata.2018.02.010.
21. Ajmal, A.; Majeed, I.; Malik, R.N.; Idriss, H.; Nadeem, M.A. Principles and mechanisms of photocatalytic dye degradation on TiO_2 based photocatalysts: A comparative overview, RSC Adv. **2014** *4* 37003–37026. doi:10.1039/c4ra06658h.
22. Galindo, C.; Jacques, P.; Kalt, A. Photodegradation of the aminoazobenzene acid orange 52 by three advanced oxidation processes: UV/H_2O_2, UV/TiO_2 and VIS/TiO_2. Comparative mechanistic and kinetic investigations, J. Photochem. Photobiol. A Chem. **2000** *130* 35–47. doi:10.1016/S1010-6030(99)00199-9.
23. Zhao, J.; Chen, C.; Ma, W. Photocatalytic Degradation of Organic Pollutants Under Visible Light Irradiation, Top. Catal. **2005** *35* 269–278. doi:10.1007/s11244-005-3834-0.
24. Maragatha, J.; Jothivenkatachalam, K.; Karuppuchamy, S. Synthesis and characterization of visible light-responsive carbon doped Ti_4O_7 photocatalyst, J. Mater. Sci. Mater. Electron. **2016** *27* 9233–9239. doi:10.1007/s10854-016-4961-z.
25. Nagalakshmi, M.; Karthikeyan, C.; Anusuya, N.; Brundha, C.; Basu, M.J.; Karuppuchamy, S. Synthesis of TiO_2 nanofiber for photocatalytic and antibacterial applications, J. Mater. Sci. Mater. Electron. **2017** *28* 15915–15920. doi:10.1007/s10854-017-7487-0.
26. Mills, A.; Davies, R.H.; Worsley, D. Water purification by semiconductor photocatalysis. Chem. Soc. Revs. **1993** *22* 417-25.
27. Wilke, K.; Breuer, H.D. The influence of transition metal doping on the physical and photocatalytic properties of titania. J. Photochem. Photobiol. A. **1999** *121* 49-53.
28. Fallah, M.; MacKenzie, K.J.D.; Hanna, J.V; Page, S.J. Novel photoactive inorganic polymer composites of inorganic polymers with copper (I) oxide nanoparticles. J. Mater. Sci. **2015** *50* 7374-83. DOI:10.1007/s10853-0153-9295-3.
29. Kabra, K.; Chaudhary, R.; Sawhney, R.L. Treatment of hazardous organic and inorganic compounds through aqueous-phase photocatalysis: A review, Ind. Eng. Chem. Res. **2004** *43* 7683–7696. doi:10.1021/ie0498551.
30. Zailan, S.N.; Bouaissi, A.; Mahmed, N.; Abdullah, M.M.A.B. Influence of ZnO Nanoparticles on Mechanical Properties and Photocatalytic Activity of Self-cleaning ZnO-Based Geopolymer Paste, J. Inorg. Organomet. Polym. Mater. **2020** *30* 2007–2016. doi:10.1007/s10904-019-01399-3.
31. Pacheco-Torgal, F.; Jalali, S. Nanotechnology: Advantages and drawbacks in the field of construction and building materials, Constr. Build. Mater. **2011** *25* 582–590. doi:10.1016/j.conbuildmat.2010.07.009.
32. Zheng, K.; Chen, L.; Gbozee, M. Thermal stability of geopolymers used as supporting materials for TiO_2 film coating through sol-gel process: Feasibility and improvement, Constr. Build. Mater. **2016** *125* 1114–1126. doi:10.1016/j.conbuildmat.2016.09.007.
33. Fan, W.; Lai, Q.; Zhang, Q.; Wang, Y. Nanocomposites of TiO_2 and reduced graphene oxide as efficient photocatalysts for hydrogen evolution, J. Phys. Chem. C. **2011** *115* 10694–10701. doi:10.1021/jp2008804.

34. Chen, L.; Zheng, K.; Liu, Y. Geopolymer-supported photocatalytic TiO_2 film: Preparation and characterization, Constr. Build. Mater. **2017** *151* 63–70. doi:10.1016/j.conbuildmat.2017.06.097.

35. Strini, A.; Roviello, G.; Ricciotti, L.; Ferone, C.; Messina, F.; Schiavi, L.; Corsaro, D.; Cioffi, R. TiO_2-based photocatalytic geopolymers for nitric oxide degradation, Materials (Basel). **2016** *9* doi:10.3390/ma9070513.

36. Bravo, P.I.; Malenab, R.A.; Shimizu, E.; Yu, D.E.; Promentilla, M.A. Synthesis of geopolymer spheres with photocatalytic activity, MATEC Web Conf. **2019** *268* 04007. doi:10.1051/matecconf/201926804007.

37. Samuneva, B.; Kozhukharov, V.; Trapalis, C.; Kranold, R. Sol-gel processing of titanium-containing thin coatings - Part I Preparation and structure, J. Mater. Sci. **1993** *28* 2353–2360. doi:10.1007/BF01151665.

38. Gasca-Tirado, J.R.; Manzano-Ramírez, A.; Villaseñor-Mora, C.; Muñiz-Villarreal, M.S.; Zaldivar-Cadena, A.A.; Rubio-Ávalos, J.C.; Borrás, V.A.; Mendoza, R.N. Incorporation of photoactive TiO_2 in an aluminosilicate inorganic polymer by ion exchange, Microporous Mesoporous Mater. **2012** *153* 282–287. doi:10.1016/j.micromeso.2011.11.026.

39. Yang, X.; Liu, Y.; Yan, C.; Peng, R.; Wang, H. Geopolymer-TiO_2 nanocomposites for photocsatalysis: Synthesis by one-step adding treatment versus two-step acidification calcination, Minerals. **2019** *9* doi:10.3390/min9110658.

40. Lertcumfu, N.; Jaita, P.; Thammarong, S.; Lamkhao, S.; Tandorn, S.; Randorn, C.; Tunkasiri, T.; Rujijanagul, G. Influence of graphene oxide additive on physical, microstructure, adsorption, and photocatalytic properties of calcined kaolinite-based geopolymer ceramic composites, Colloids Surfaces A Physicochem. Eng. Asp. **2020** *602* 125080. doi:10.1016/j.colsurfa.2020.125080.

41. Gupta, K.; Khatri, O.P. Reduced graphene oxide as an effective adsorbent for removal of malachite green dye: Plausible adsorption pathways, J. Colloid Interface Sci. **2017** *501* (2017) 11–21. doi:10.1016/j.jcis.2017.04.035.

42. Gao, Y.; Wu, J.; Ren, X.; Tan, X.; Hayat, T.; Alsaedi, A.; Cheng, C.; Chen, C. Impact of graphene oxide on the antibacterial activity of antibiotics against bacteria, Environ. Sci. Nano. **2017** *4* 1016–1024. doi:10.1039/c7en00052a.

43. Gopalakrishnan, A.; Krishnan, R.; Thangavel, S.; Venugopal, G.; Kim, S.J. Removal of heavy metal ions from pharma-effluents using graphene-oxide nanosorbents and study of their adsorption kinetics, J. Ind. Eng. Chem. **2015** *30* 14–19. doi:10.1016/j.jiec.2015.06.005.

44. Shamsaei, E.; de Souza, F.B.; Yao, X.; Benhelal, E.; Akbari, A.; Duan, W. Graphene-based nanosheets for stronger and more durable concrete: A review, Constr. Build. Mater. **2018** *183* 642–660. doi:10.1016/j.conbuildmat.2018.06.201.

45. Zhang, Y.J.; Yang, M.Y.; Zhang, L.; Zhang, K.; Kang, L. A new graphene/geopolymer nanocomposite for degradation of dye wastewater, Integr. Ferroelectr. **2016** *171* 38–45. doi:10.1080/10584587.2016.1171178.

46. Zhang, Y.J.; He, P.Y.; Zhang, Y.X.; Chen, H. A novel electroconductive graphene/fly ash-based geopolymer composite and its photocatalytic performance, Chem. Eng. J. **2018** *334* 2459–2466. doi:10.1016/j.cej.2017.11.171.

47. Zheng, Z.; Huang, B.; Wang, Z.; Guo, M.; Qin, X.; Zhang, X.; Wang, P.; Dai, Y. Crystal faces of Cu_2O and their stabilities in photocatalytic reactions, J. Phys. Chem. C. **2009** *113* 14448–14453. doi:10.1021/jp904198d.

48. Huang, L.; Peng, F.; Yu, H.; Wang, H. Preparation of cuprous oxides with different sizes and their behaviors of adsorption, visible-light driven photocatalysis and photocorrosion, Sol. St. Sci. **2009** *11* 129-138 doi:10.1016/j.solidstatesciences.2008.04.013.

49. Fallah, M.; MacKenzie, K.J.D.; Hanna, J.V.; Page, S.J. Novel photoactive inorganic polymer composites of inorganic polymers with copper(I) oxide nanoparticles, J. Mater. Sci. **2015** *50* 7374–7383. doi:10.1007/s10853-015-9295-3.

50. Saleh, T.A. Syntheses and Applications of Carbon Nanotubes and Their Composites, **2013**. doi:10.5772/3377.

51. Singh, N.B.; Saxena, S.K.; Kumar, M. Effect of nanomaterials on the properties of geopolymer mortars and concrete, in: Mater. Today Proc., Elsevier, **2018:** pp. 9035–9040. doi:10.1016/j.matpr.2017.10.018.

52. Mahmoodi, N.M. Synthesis of magnetic carbon nanotube and photocatalytic dye degradation ability, Environ. Monit. Assess. **2014** *186* 5595–5604. doi:10.1007/s10661-014-3805-7.

53. Bi, S.; Liu, M.; Shen, J.; Hu, X.M.; Zhang, L. Ultrahigh Self-Sensing Performance of Geopolymer Nanocomposites via Unique Interface Engineering, ACS Appl. Mater. Interfaces. **2017** *9* 12851–12858. doi:10.1021/acsami.7b00419.

54. Huang, L.; Peng, F.; Wang, H.; Yu, H.; Li, Z. Preparation and characterization of Cu_2O/TiO_2 nano-nano heterostructure photocatalysts, Catal. Commun. **2009** *10* 1839–1843. doi:10.1016/j.catcom.2009.06.011.

55. Falah, M.; MacKenzie, K.J.D. Synthesis and properties of novel photoactive composites of P25 titanium dioxide and copper (I) oxide with inorganic polymers, Ceram. Int. **2015** *41* 13702–13708. doi:10.1016/j.ceramint.2015.07.198.

56. Falah, M.; MacKenzie, K.J.D.; Knibbe, R.; Page, S.J.: Hanna, J.V. New composites of nanoparticle Cu (I) oxide and titania in a novel inorganic polymer (geopolymer) matrix for destruction of dyes and hazardous organic pollutants, J. Hazard. Mater. **2016** *318* 772–782. doi:10.1016/j.jhazmat.2016.06.016.

57. Zailan, S.N.; Bouaissi, A.; Mahmed, N.; Abdullah, M.M.A.B. Influence of ZnO Nanoparticles on Mechanical Properties and Photocatalytic Activity of Self-cleaning ZnO-Based Geopolymer Paste, J. Inorg. Organomet. Polym. Mater. **2020** *30* 2007–2016. doi:10.1007/s10904-019-01399-3.

58. Zhang, Y.J.; He, P.Y.; Yang, M.Y.; Chen, H.; Liu, L.C. Renewable conversion of slag to graphene geopolymer for H_2 production and wastewater treatment, Catal. Today. **2019** doi:10.1016/j.cattod.2019.02.003.

59. Zhang, Y.J.; He, P.Y.; Chen, H. A novel CdO/graphene alkali-activated steel slag nanocomposite for photocatalytic degradation of dye wastewater, Ferroelectrics. **2018** *522* 1–8. doi:10.1080/00150193.2017.1391587.

60. Saufi, H.; El Alouani, M.; Alehyen, S.; El Achouri, M.; Aride, J.; Taibi, M. Photocatalytic degradation of methylene blue from aqueous medium onto perlite-based geopolymer, Int. J. Chem. Eng. **2020** 9498349. https://doi.org/10.1155/2020/9498349

61. Zhang, Y.J.; Liu, L.C. Fly ash-based geopolymer as a novel photocatalyst for degradation of dye from wastewater, Particuology **2013** *11* 353-8. https://doi.org/10.1016/j.partic.2012.10.007.

62. He, P.Y.; Zhang, Y.J.; Chen, H.; Liu, L.C. Development of an eco-efficient $CaMoO_4$/electroconductive geopolymer composite for recycling silicomanganese slag and degradation of dye wastewater, J. Clean. Product. **2019** *208* 1476-1487 https://doi.org/10.1016/j.jclepro.2018.10.176.